Analysis of inhomogeneous Ge/SiC heterojunction diodes.

P. M. Gammon[1], A. Pérez-Tomás[3], V. A. Shah[2], G. J. Roberts[1], M. R. Jennings[1], J. A. Covington[1] and P. A. Mawby[1].
[1]*School of Engineering, University of Warwick, Coventry, CV4 7AL, United Kingdom*
[2]*Department of Physics, University of Warwick, Coventry, CV4 7AL, United Kingdom and*
[3]*Centre Nacional de Microelectrónica (CNM-CSIC) Campus UAB, 08193 Barcelona, Spain*
(Dated: September 29, 2009)

In this article Schottky barrier diodes comprising of a *n*-*n* Germanium-Silicon Carbide (Ge-SiC) heterojunction are electrically characterised. Circular transmission line measurements prove that the nickel front and back contacts are ohmic, isolating the Ge/SiC heterojunction as the only contributor to the Schottky behaviour. Current-voltage plots taken at varying temperature (IVT) reveal that the ideality factor (n) and Schottky barrier height (Φ) are temperature dependent and that incorrect values of the Richardson constant (A^{**}) are being produced, suggesting an inhomogeneous barrier. Techniques originally designed for metal-semiconductor SBH extraction are applied to the heterojunction results to extract values of Φ and A^{**} that are independent of temperature. The experimental IVT data is replicated using the Tung model. It is proposed that small areas, or patches, making up only 3% of the total contact area will dominate the I-V results due to their low SBH of 1.033 eV. The experimental IVT data is also analysed statistically using the extracted values of Φ to build up a Gaussian distribution of barrier heights, including the standard deviation and a mean SBH of 1.126 eV, which should be analogous to the SBH extracted from capacitance-voltage (C-V) measurements. Both techniques yield accurate values of A^{**} for SiC. However, the C-V analysis did not correlate with the mean SBH as expected.

PACS numbers: Valid PACS appear here

I. INTRODUCTION

Silicon Carbide (SiC) is the material of choice for modern power semiconductor applications, having a superior reverse breakdown voltage and a low specific on-resistance when compared to Silicon (Si). SiC Schottky Barrier Diodes (SBD) have become commercially available[1]. Epitaxially growing a thin layer of Germanium (Ge) on the SiC surface has been shown[2] to reduce the turn-on voltage of SBD devices to approximately 0.3V, while maintaining a relatively low leakage current for applications where on-state and switching losses must be kept to the minimum. A further reduction in leakage current could be attained using Junction Barrier Schottky diodes structures[3].

Further motivation in researching these heterostructures is the need to reduce the number of interface traps at the SiC/SiO2 interface of a SiC MOS structure. The use of an epitaxial layer of Si was proposed[4–7] which would have the added benefit of greatly increasing the channel mobility. This has progressed to Ge, due to the material's even higher mobility (especially in p-type where the hole mobility is 5 times that of Si and 21 times that of SiC) and its compatibility with high-K dielectrics.

In measuring the Schottky Barrier Height (SBH) of the Ge/SiC hetero-structures using Capacitance-Voltage (C-V) and current-voltage (I-V) analyses, a discrepancy occurred, with the C-V value exceeding the I-V value. This suggested inhomogeneity at the Ge/SiC heterojunction interface, similar to several metal-semiconductor studies over the last two decades[8–18]. Inhomogeneities are imperfections at the interface between two materials. These are borne from the surface not being atomically flat due to grain boundaries, multiple phases, facets, defects etc[8]. Other sources of inhomogeneity include non-uniformity within the doping profile[9] and residual materials left over from processing[10] creating interfacial states between the surfaces.

Inhomogeneity at the interface of two materials causes spatial fluctuations in the SBH to occur. Against a background of uniform SBH, patches of varying SBH are present[11–13], the size of which are considered to be small compared to the depletion width of the semiconductor[14]. Over an entire contact, the SBH is assumed to have a Gaussian distribution with a standard distribution (σ_s) about a mean SBH value (Φ_0).[8,9,11,12,15,16] Given this, many patches exist with a SBH significantly lower than the mean value explaining the I-V and C-V analysis discrepancy. When finding a path through the interface of the two materials, the carriers choose the path with the lowest barrier to overcome, the result being that the I-V analysis yields a barrier height (Φ_{IV}) that is lower than Φ_0. C-V analysis considers an average SBH value (Φ_{CV}) over the whole interface, therefore this value is very likely to be closer to Φ_0[9,15]. Ballistic electron emission microscopy on Pd/6H-SiC barriers, has recently confirmed the presence of a nanometer scale distribution of SBH[19], whilst conductive atomic force microscopy has also been used to map inhomogeneities on Au/4H-SiC samples[20].

The origins of inhomogeneous Schottky barrier theory dates back to the 1960's when non-linearities within the classic Richardson plot hindered the extraction of the SBH and Richardson constant (A^{**}).[21] This became known as the T_0 effect whereby it was found that adding a temperature constant into the thermionic emission equation the plot would linearise and aid in the extraction of the SBH. We now know that at an inhomogeneous interface, the SBH will rise and the ideality factor fall as the

temperature is increased due to the junction current becoming dominated by fewer low SBH patches[11–13]. The relationship between the SBH and the ideality factor with varying temperature forms a linear relationship. When this is extrapolated to an ideality factor of 1, the average SBH $\left(\Phi_B^0\right)$ can be extracted[17]. Φ_B^0 is an ideal value which would be the SBH of a spatially homogeneous interface. Therefore, it can be considered a maximum SBH value for real, inhomogeneous interfaces.

The temperature dependence of the SBH causes the non-linearity in Richardson Plots. Many solutions were suggested to return linearity to the plots[21–23] before the link with inhomogeneities was made[9,11,15,24]. Two techniques exist to modify the classic Richardson plot to extract the barrier height, taking into account SBH lowering due to an inhomogeneous contact. The first involves extracting the barrier height relevant to I-V analyses, a value referred to as the effective barrier height (Φ_{eff}). The second uses Gaussian statistics to extract an average barrier height (Φ_0), a value that is considered close to that extracted by C-V analysis[9,15].

To extract Φ_{eff} a theoretical model is created based on the thermionic emission equation that replicates real I-V plots taken at different temperatures. Within the model the area of the diode A is replaced with the product NA_{eff} where A_{eff} is an area (or patch) of low SBH, and N is the number of them in an area A. A fit almost identical to the real data can be achieved, and by using a modified Richardson Plot, Φ_{eff} is attained and (A^{**}) can be extracted. This is based on work by Roccaforte et al[10], which in turn is based on Tung's model[11–13].

The second technique uses Gaussian statistics to relate experimental values of SBH extracted from I-V analysis, Φ_{IV}, back to the mean SBH, Φ_0. A value for the standard deviation of the patches' SBH is extracted from the experimental data before this is used to modify the Richardson plot. This is a method first described in the paper by Song et al[15] and further built on by Werner and Güttler[9].

In this paper we will show that the solutions to problems associated with inhomogeneous metal-semiconductor Schottky contacts can similarly be applied to inhomogeneous heterojunction Schottky contacts. We will show that the front and back contacts of the Ge/SiC heterojunction diodes are ohmic, proving that the only rectifying behaviour comes from the Ge/SiC interface. The two techniques previously described will then be used to attain the SBH values. We will then compare these theoretical results to the I-V and C-V results.

II. EXPERIMENTAL DETAILS

An n-type (0001) Si face, 4^o off axis, 4H-SiC wafer was purchased from Cree Inc with a 10 μm, lightly n-type doped ($1.4 \times 10^{15} cm^{-3}$), epitaxial layer. This was diced into 10×10 mm samples before germanium films were deposited using V100S Molecular Beam Epitaxy (MBE) system. Prior to deposition, the wafer was cleaned using a RCA2 clean[25] (H_2O:HCl:H_2O_2, 5:1:1) followed by a hydrofluoric acid dip to remove the oxide formed during the RCA2 process. This cleaning process has been demonstrated[5] to be of high quality, providing minimal reverse leakage current. This was followed by a high temperature bake within the MBE system to desorb the native oxide and any other contaminants. N-type highly doped germanium (HD-Ge) layers ($N_{D,Ge} = 5 \times 10^{19} cm^{-3}$), 300 nm in thickness, were deposited at a rate of 0.1 $\mathring{A}s^{-1}$ with antimony as the dopant at a temperature of 500^oC. With the Ge being highly doped, it is expected that Nickel (Ni) will form a good ohmic contact with the Ge. In a similar situation, Ni has been shown[26] to form a low-resistance ohmic contact with Ge on a gallium arsenide substrate. 400 nm of Ni was sputtered onto the Ge surfaces. The resulting layer was then patterned and etched into circular transmission line measurement (CTLM) structures and dots 200 μm and 400 μm in diameter. The dots, though not the CTLM structures, were then formed into mesa diode structures by etching the remaining Ge, whilst the CTLM structures were protected from this step. This is illustrated in the inset of Fig. 1. Similarly, a back contact with CTLM structures were formed by sputtering Ni onto the back SiC surface where the doping is higher ($1 \times 10^{18} cm^{-3}$). The structures were further annealed at 450^oC in nitrogen ambient for 5 minutes.

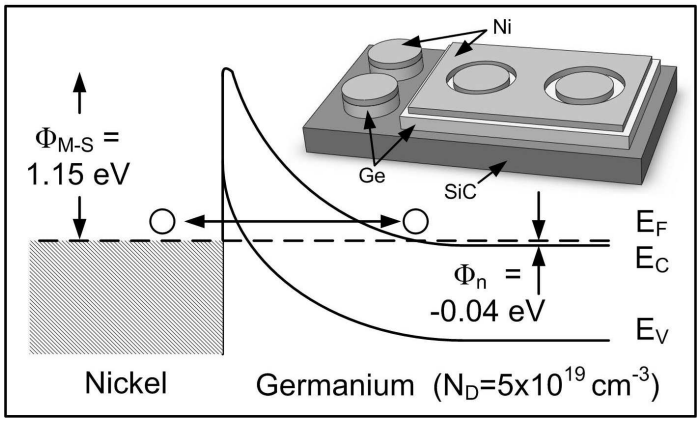

FIG. 1: The Ni-Ge band structure. Inset: A 3-dimensional view of the three layers that make up the CTLM structures and the mesa etched diode pads.

Prior to nickel deposition, C-V measurements were taken at room temperature directly on the MBE deposited germanium. This was carried out using an Agilent Technologies B1500A Semiconductor Device Analyzer connected to a Materials Development Corporation 802-200 mercury probe.

Post-processing, the diodes were subject to I-V analysis at varying temperature (IVT), from -50^{o}C to 175^{o}C (225-450 K) at 25^{o}C intervals. With the diodes placed in a Tenney environmental chamber, wire bonding di-

rectly to the nickel dots allowed heat proof wires to be run out to the Agilent Semiconductor Device Analyzer, which carried out and recorded the tests. The temperature was controlled and monitored in the chamber by a Watlow Series 942 temperature controller, though this was verified using a Fluke 52 II Thermometer.

III. RESULTS AND DISCUSSION

A. Ohmic Contacts

The front and back contacts of Ni-Ge and Ni-SiC respectively can be proven to be ohmic, thus isolating the Ge/SiC heterojunction as the only contributor to the Schottky behaviour of the structures. The band structure of the Ni-Ge front contact can be seen in Fig. 1; the Ni-SiC back contact would be lain out in a very similar fashion. The high doping of the Ge leads to a degenerate semiconductor whereby the fermi level (E_F) exceeds the conduction band (E_C). The theoretical Ni-Ge barrier height (Φ_{M-S}) is 1.15 eV. The high doping is the cause of a very thin depletion width, thin enough to allow electrons to quantum-mechanically tunnel through the barrier, a conduction mechanism referred to as Field Emission (FE). With lower doped semiconductors, the usual path for electrons is to be thermally excited over the barrier, known as Thermionic Emission (TE). A middle ground exists whereby carriers are excited to a level where they can tunnel through a thinner barrier, known as Thermionic-Field Emission (TFE).

Concentrating on the Ni/Ge front contact, the relevant conduction method can be calculated as well as the effective barrier height. To determine the conduction method, the characteristic tunnelling energy E_{00} of the semiconductor can be calculated and compared with the thermal energy kT. E_{00} is given by[27]

$$E_{00} = \frac{q\hbar}{2}\sqrt{\frac{N_d}{m_T^* \epsilon_s}} \tag{1}$$

where $\hbar$ is the reduced Planck's constant, N_d is the N-type doping, m_T^* is the tunnelling effective mass and ϵ_s is the permittivity of the semiconductor. m_T^* is given[28] for n-type Ge as $0.12m_0$, whilst the dielectric constant is $16e_0$. FE is said to dominate[29] if $E_{00} \geq 5kT$ whereas TE will dominate at $E_{00} \leq 0.5kT$, and between these margins TFE will dominate. E_{00} for the HD-Ge is between 2.5 and 5 times larger than kT over the 225-450 K range of temperatures. This means that it will be on the border of TFE and FE. The barrier peak value of tunnelling (E_m) during TFE is given by[27,30]

$$E_m = \frac{q\left(\Phi_{M-S} - \Phi_n - V_F\right)}{\cosh^2\left(E_{00}/kT\right)} \tag{2}$$

where Φ_n is the energy difference between E_C and E_F shown in Fig. 1 and V_F is the applied forward voltage. At 450K, E_m is calculated to be 35 meV above the conduction band, hence it is fair to presume that FE dominates this metal-semiconductor contact. At 225 K this peak is at only 0.25 meV above the conduction band. Thermionic emission provides a path of lowest resistance, hence the resistance over the ohmic Ni-Ge barrier will be at its lowest at high temperature. However, as will be shown next, the measured values of contact resistance over this barrier are so low that the difference due to the temperature is minimal.

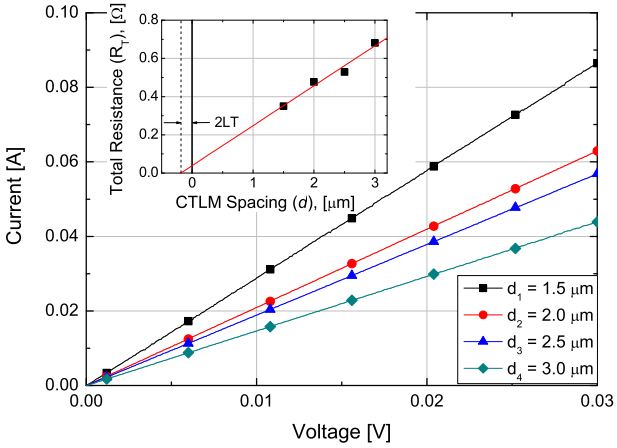

FIG. 2: I-V curves from the Ni-Ge top contact CTLM structures with varying d spacing. Inset: The extraction of the transfer length L_T.

Circular Transmission Line Measurements (CTLM) have been used to extract the contact resistance (ρ_c) of the Ni-Ge and Ni-SiC contacts and hence confirm their ohmicity. I-V measurements on each of the CTLM structures, as seen in Fig. 2, allows the extraction of the total measured resistance (R_T). The sheet resistance of each CTLM structure (R_{sh}) is then determined from R_T as follows,[29,31]

$$\frac{2\pi R_T}{R_{sh}} = \frac{L_T}{L}\frac{I_0\left(L/L_T\right)}{I_1\left(L/L_T\right)} + \frac{L_T}{L+d}\frac{K_0\left(L/L_T\right)}{K_1\left(L/L_T\right)} + \ln\left(1+\frac{d}{L}\right) \tag{3}$$

where I and K are the modified Bessel functions of the first order, L is the radius of the inner CTLM pad and d is the distance of the gap between the concentric circular pads. The transfer length (L_T) is determined graphically by plotting R_T against d for each structure as seen in the inset of Fig. 2. ρ_c can then be determined by the relationship[31]

$$L_T = \sqrt{\frac{\rho_c}{R_{sh}}}. \tag{4}$$

The contact resistance of the Ni-Ge front contact and the Ni-SiC back contact were 3×10^{-4} and 1×10^{-3} Ωcm^2

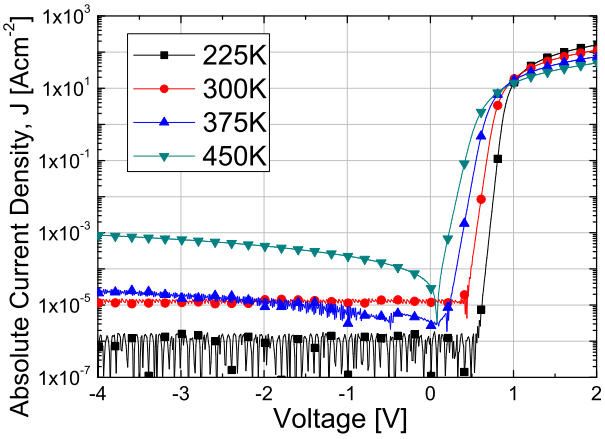

FIG. 3: Current-Voltage results from the Ge/SiC heterojunction diode taken at varying temperature.

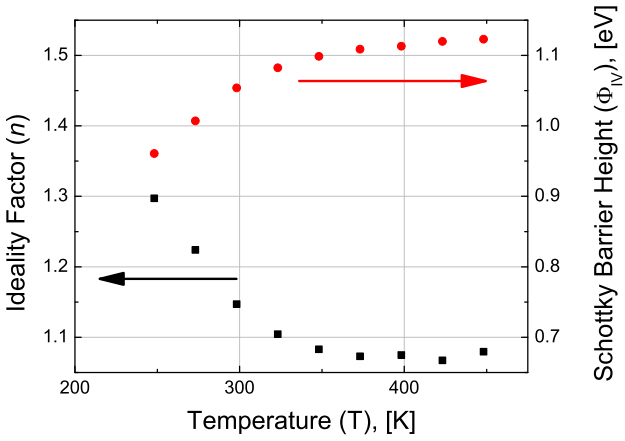

FIG. 4: The temperature dependence of the ideality factor and SBH from a Ge/SiC heterojunction diode

respectively, values consistent with previously reported values[32].

B. n-n Ge/SiC Heterojunction Schottky Contact

The IVT results showing the diode's rectifying nature at varying temperature can be seen in Fig. 3. Having proved the ohmicity of the front and back contacts it is clear that only the Ge/SiC heterojunction contributes to the rectifying Schottky behaviour. In this section, SBH and Richardson constant values will be extracted using the various techniques introduced earlier to modify the Richardson plot towards linearity. These results will be compared with each other and with the values extracted from I-V and C-V analysis.

1. *The extraction of the barrier height via I-V analysis*

Applying Eq. 1 to the lightly doped SiC epitaxial layer produces a value of E_{00} at least 50 times smaller than kT over the temperature range, indicating that the current mechanism will be TE. Furthermore, Eq. 2 indicates that tunneling could only occur 0.2 meV from the peak of the barrier. The current over this barrier will hence be dictated by the TE equation[29,30],

$$I = AA^{**}T^2 e^{-\beta\Phi_{IV}}\left(e^{\beta V/n} - 1\right) \tag{5}$$

where A is the contact area, A^{**} is the Richardson's Constant, T is the Temperature, Φ_{IV} is the barrier height specific to I-V analysis, β is the inverse thermal energy ($\beta = q/kT$) and n is the ideality factor. This can be shortened to,

$$I = I_s\left(e^{\beta V/n} - 1\right) \tag{6}$$

where I_s is the saturation current defined as

$$I_s = AA^{**}T^2 e^{-\beta\Phi_{IV}}. \tag{7}$$

I_s can be determined from log(I)-V plots by extrapolating the linear region of the plot to $V = 0$.[29].

From Eq. 5 the values of A, A^{**}, T and β are all known prior to any testing. Φ_{IV} and n can both be determined from a single I-V plot, however, the temperature dependence of both dictate that the value extracted will only be accurate at the temperature of measurement. This dependency is evident when analysing the results of the I-V measurements taken from the SiC-Ge heterojunction diode, which were recorded at 25^{o}C intervals from -50^{o}C to 175^{o}C. Fig. 4 shows how the ideality factor decreases and Φ_{IV} increases with increasing temperature over the range tested. At 25^{o}C, the ideality factor of this device was 1.035 proving that it is a contact of good quality. Φ_{IV} at 25^{o}C is 1.12 eV.

Plotting the barrier heights against their respective ideality factors as shown in Fig. 5 displays the linear correlation between the two. Extrapolating a linear fit of the data to $n = 1$ reveals the average barrier height Φ_B^0. Schmitsdorf et al[17] first reported this relationship, referring to the average barrier height as the homogeneous barrier height, the SBH that would be extracted from an ideal contact. Extrapolation to $n = 1$ in Fig. 5 provides an average barrier height of $\Phi_B^0 = 1.163$ eV.

Another technique used to extract the barrier height is via a Richardson plot, with $\ln\left(J_s/T^2\right)$ plotted against the inverse temperature, where $J_s = I_s/A$. Fig. 6 shows the Richardson plot for the SiC-Ge heterojunction diode

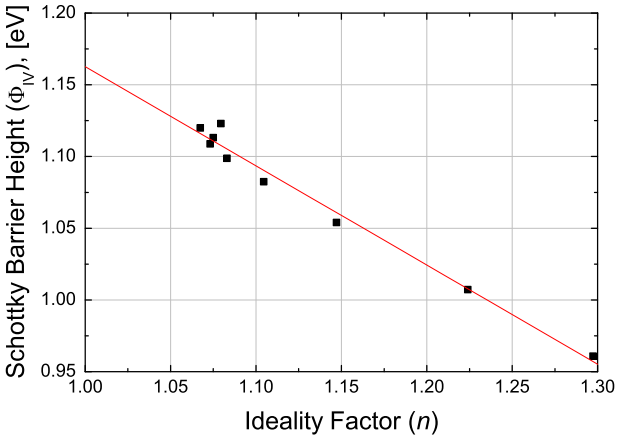

FIG. 5: With the barrier height plotted against the ideality factor, the extrapolation to $n = 1$ via a linear fit gave the average barrier height $\phi_B^0 = 1.163$

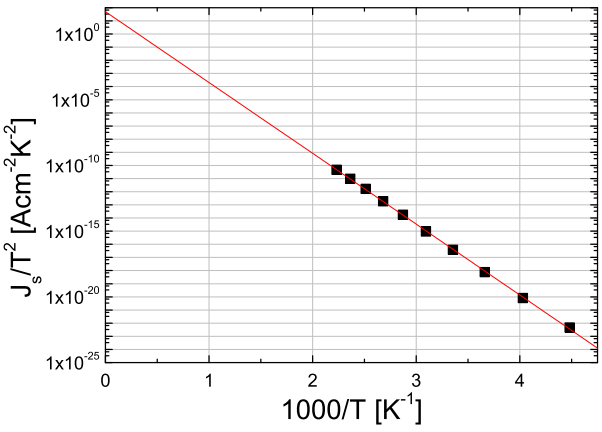

FIG. 6: An unmodified Richardson plot, $\ln\left(J_s/T^2\right)$ vs $1000/T$. A SBH, Φ_{AP}, of 1.069 eV was extracted from the slope of the linear fit, which also produced a Richardson constant of 50.368 $Acm^{-2}K^{-2}$ from the Y-intercept.

where the apparent SBH, Φ_{AP}, was found to be 1.069 eV, and the Richardson constant A^{**} extracted from the Y-intercept was 50.368 $Acm^{-2}K^{-2}$. As mentioned previously, the temperature dependence of Φ_{IV} leads to erroneous results from the Richardson plot with the Richardson constant approximately one third that of the calculated figure[33] of 146 $Acm^{-2}K^{-2}$, though the method for calculating this value has been disputed[34].

It is therefore necessary to use other techniques that facilitate the extraction of temperature independent values, taking into account the patches of low SBH hidden amongst the high SBH.

2. *The extraction of the effective barrier height*

This method of extracting the SBH presumes that within an inhomogeneous contact, the distribution of low SBH patches that contribute to I-V analysis can be represented by one common SBH, Φ_{eff}, and that all the current passing through the device does so only over these patches. The value Φ_{eff} is representative of the SBH whenever the diode is being used in any practical situation.

Considering the TE equation (Eq. 5), the area A can be replaced by the product NA_{eff} which represents the total area of a contact made up of low SBH. Individually, N is the number of patches in the area A and A_{eff} is the area of a single patch of low SBH. Eq. 5 can be rewritten substituting in the product NA_{eff},

$$J = NA_{eff}A^{**}T^2e^{-\beta\Phi_{eff}}\left(e^{\beta V/n} - 1\right). \qquad (8)$$

where the SBH modelling parameter, Φ_{eff} replaces Φ_{IV}. We can use Eq. 8 to simulate the experimental IVT curves of Fig. 3. The calculated figure[33] of A^{**}, 146 $Acm^{-2}K^{-2}$ is presumed correct in this method, leaving A_{eff}, N, Φ_{eff} and n as variables in Eq. 8. A_{eff} is also dependent on the value of Φ_{eff}, being defined[11,13] as

$$A_{eff} = \frac{4\pi\eta}{9\beta V_{bb}}\left(\Phi_B^0 - \Phi_{eff}\right) \qquad (9)$$

where V_{bb} is the band bending at the Ge/SiC interface and $\eta = \varepsilon_s/qN_D$. Hence, three parameters can be used to manipulate a theoretical fit of the IVT data. Fig. 7 shows graphically how altering each of these variables affects these plots. Increasing the number of low SBH patches, N, allows more current to pass through the device for the same voltage and hence the fits move upwards. Increasing the SBH, Φ_{eff}, causes a reduction in the current flowing over the barrier, hence a vertical drop in the fits, however, being an exponential term, all the temperature fits also spread out away from each other. Increasing the ideality factor, n, causes the resistance of the device to increase, thus decreasing the gradient of the slope.

Fig. 7 shows that selecting the correct balance of the variables N, Φ_{eff} and n, provides a very good approximation to the linear fits of the experimental data. The values of n used were those extracted from each individual I-V plot, as was illustrated in Fig. 4. The values of Φ_{eff} and N were arrived at by using a modified Richardson Plot. To remove the temperature dependence on the SBH within a Richardson plot, the total area dominated by the low SBH patches (NA_{eff}) is taken into consideration within the Richardson plot, Eq. 8 rearranging to

$$\ln\left(\frac{J_s}{T^2NA_{eff}}\right) = \ln\left(A^{**}\right) - \frac{q\Phi_{eff}}{kT}. \qquad (10)$$

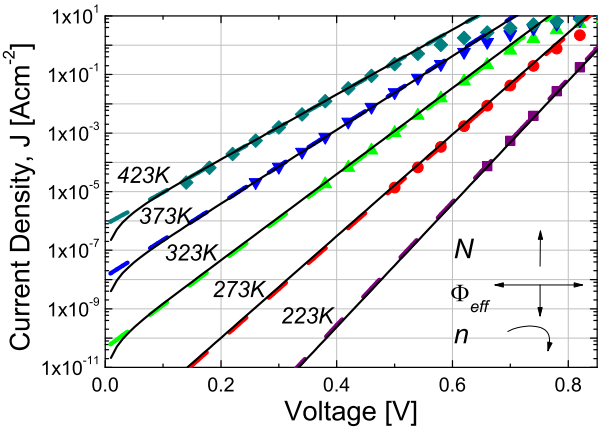

FIG. 7: A graphical indication of how a theoretical model based on Eq. 8 can be used to simulate experimental data. The scattered shapes are experimental data extracted from IVT measurements. The dashed lines are linear fits of the experimental data extrapolated to Y=0. The solid black lines are the theoretical fits from Eq. 8. The effect of altering the parameters N, Φ_{eff} and n in Eq. 8 are also shown.

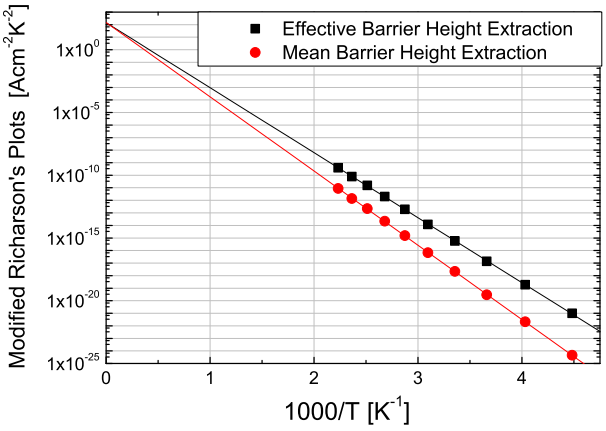

FIG. 8: The modified Richardson plots for the extraction of the effective SBH, Φ_{eff}, and the Mean SBH, Φ_0, are respectively, $\ln\left(J_s/T^2NA_{eff}\right)$ and $\ln\left(J_s/T^2\right)-0.5\beta^2\sigma^2$ vs $1000/T$. An effective barrier height of 1.033 eV and a mean barrier height of 1.126 eV were extracted.

Once the fit is close to being correct, the value of Φ_{eff} extracted from the Richardson Plot is fed back into the theoretical model, producing a tighter fit and a more accurate Richardson constant. Using this method, Φ_{eff} was found to be 1.033 eV and N was 1.1×10^7. As a result, at 25^{o}C, A_{eff} was found to be 2.9×10^{-9} cm^2 and the product NA_{eff} represented 3% of the total area A. The resulting modified Richardson Plot can be seen in Fig. 8. The Richardson constant extracted was 145.6 $Acm^{-2}K^{-2}$.

3. *The extraction of the mean barrier height*

The SBH extracted from this technique is analogous to that extracted from C-V analysis[9,15], that is, an average of the barrier heights over the entire contact, with no SBH of any size contributing any more than any other. The value extracted is hence known as the mean SBH, Φ_0.

The amount of patches (dn) that will have SBH values falling between Φ_0, and the value of SBH measured from the individual I-V curves Φ_{IV}, has a Gaussian distribution given by[9,15]

$$\mathrm{d}n = \frac{N}{\sigma\sqrt{2\pi}} \exp\left[-\frac{\left(\Phi_0 - \Phi_{IV}\right)^2}{2\sigma^2}\right] \mathrm{d}\Phi_0. \qquad (11)$$

where σ is the standard deviation of the distribution and N the total number of patches in the area A. Song et al[15] show that the total forward current can be given by multiplying Eqs. 5 and 11, and integrating, giving

$$I = AA^{**}T^2 e^{-\beta\Phi_{IV}+0.5\beta^2\sigma^2}\left(e^{\beta V/n}-1\right). \qquad (12)$$

The thermionic emission equation for current over the barrier Φ_0 is

$$I = AA^{**}T^2 e^{-\beta\Phi_0}\left(e^{\beta V/n}-1\right). \qquad (13)$$

Combining Eqs. 12 and 13 and rearranging leaves

$$\Phi_{IV} = \Phi_0 - \frac{\beta\sigma^2}{2}. \qquad (14)$$

This allows the values of SBH measured from the I-V analysis to be plotted against the inverse thermal energy, to extract σ and Φ_0. This is shown in Fig. 9 where σ was found to be 0.0384 eV. The value of Φ_0 extracted was 1.127 eV. Verification of this value can be carried out using a Richardson plot after Eq. 12 has been rearranged to

$$\ln\left(\frac{J_s}{T^2}\right) - \left(\frac{\beta^2\sigma^2}{2}\right) = \ln\left(A^{**}\right) - \frac{q\Phi_0}{kT}. \qquad (15)$$

Fig. 8 shows the resulting Richardson Plot where Φ_0 was found to be 1.126 eV and A^{**} was 143.5 $Acm^{-2}K^{-2}$.

4. *The extraction of the barrier height via C-V analysis*

Capacitance-voltage (C-V) measurements were carried out on the heterojunction structure prior to nickel deposition in order to extract the SBH value, Φ_{CV} of the

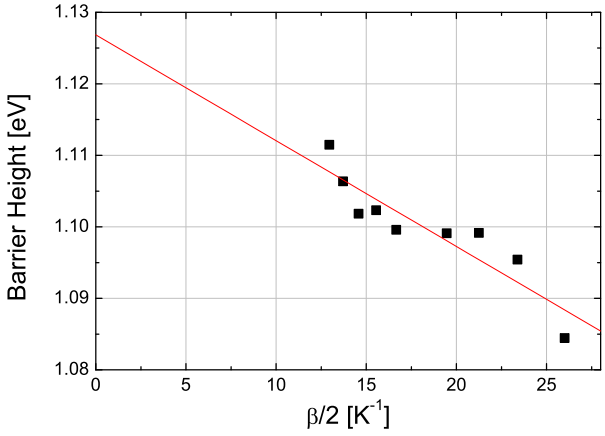

FIG. 9: The barrier heights extracted from I-V analsysis plotted against the inverse thermal energy. Φ_0 is 1.127 eV and σ is 0.0384 eV.

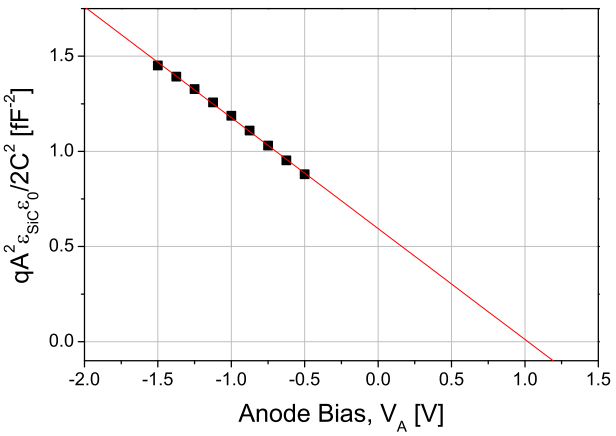

FIG. 10: A conventional CV plot used to extract a built in potential of 1.025 eV and a substrate doping of $N_D = 1.72 \times 10^{15}\ cm^{-2}$

Ge/SiC interface. Given that the unit area of a Schottky diode is given by[29,35],

$$\frac{C}{A} = \sqrt{\frac{qN_D\varepsilon_0\varepsilon_{SiC}}{2\left(V_{bi} - V_A\right)}}, \tag{16}$$

a plot of $1/C^2$ against the applied voltage V_A leads to the extraction of the built-in potential V_{bi} from the point $x = 0$. Figure 10 shows the C-V results for the SiC-Ge heterojunction diode where V_{bi} was found to be 1.025 eV and the substrate doping of $N_D = 1.72 \times 10^{15}\ cm^{-2}$ is very close to the manufacturers specification of $N_D = 1.4 \times 10^{15}\ cm^{-2}$. V_{bi} can be used to give Φ_{CV} using

$$\Phi_{CV} = V_{bi} + V_{0,SiC} - V_{0,Ge}, \tag{17}$$

where $V_{0,SiC}$ and $V_{0,Ge}$ is the potential difference between the conduction band and Fermi level of SiC and Ge respectively. These values are 0.239 eV and -0.039 eV respectively, $V_{0,Ge}$ being negative due to its degeneracy[30]. This leads to a value of Φ_{CV} of 1.303 eV.

5. *A comparison of the results*

Inhomogeneities are common place at metal-semiconductor Schottky barriers mainly due to the processes involved. Metal deposition, usually sputtering, and subsequent annealing produce a patched interface containing a mix of species and alloys[8–10]. Representative of this is the well known Ni-Ti based contact structure on 4H-SiC[36,37]. Nickel and titanium silicides are reported to form in a random, non-uniform fashion over the entire contact.

The MBE growth of a Ge layer is presumed to be a better way of controlling the barrier height due to a more uniform growth distribution. In addition, annealing at relatively low temperature (450^{o}C) results in a reduced reaction of the species at the Ge/SiC interface. However, despite these more favourable conditions, the experimental results have proven that inhomogeneities also play a major role on the practical behaviour of the heterojunction diode.

Here, the varying techniques used to extract the SBH produced an array of different results. The spread of these results can be seen in Fig. 11 along with the effective area that each SBH occupies as a percentage of the total contact area A. The average barrier height Φ_B^0, is representative of a SBH from an ideal ($n = 1$), homogeneous diode[17] and as such, one would expect a uniform barrier height over the interface, with no patches of low SBH. As such, the value of Φ_B^0 should represent a theoretical SBH maximum for the diode in question. Indeed, with the exception of Φ_{CV}, the SBH values fall in line beneath this value. The unmodified Richardson Plot yields Φ_{AP}, a value skewed due to the absence of any temperature compensation, but located at the lower end of the theoretical SBH distribution, Φ_0. As expected, the effective barrier height, Φ_{eff} a product of only 3% of the total contact area produces the lowest SBH at 1.033 eV due to the current transport over only the lowest barriers. Φ_{eff} can be considered the most relevant of the SBH values as it demonstrates what happens when the diode is being used in its day-to-day application. This was demonstrated in Fig. 7, where Φ_{eff} was employed to produce an accurate fit to the experimental IVT data.

The theory[9,15] indicates that the values of Φ_{CV} and Φ_0 values should be similar if not identical as the statistical measures employed in calculating the mean SBH should compensate for the patches of low SBH. However, there are practical realities that must be taken into account

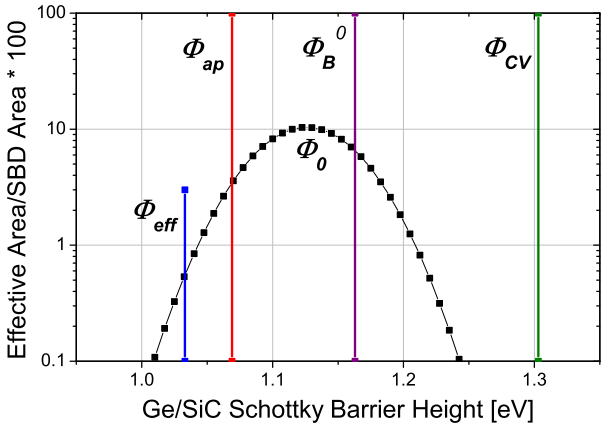

FIG. 11: A comparison of the SBH extraction techniques, showing the effective area percentage that each barrier height occupies within the total area A.

that may suggest why the two do not exactly correlate.

The C-V measurements were carried out prior to Ni deposition using a mercury probe directly to the Ge rather than probing directly to the post-processed Ni to reduce the series resistance from the measuring equipment. However, using mercury to probe to the Ge may have affected the result gained due to it having a lower work function of 4.49 eV compared to nickel's 5.15 eV. This may have had a knock on effect on the SBH between the Ni and Ge due to the amount of band bending the metal induces.

One must also consider the distribution of the SBHs. It cannot be discounted that this distribution could in fact be more top heavy, with more patches of high SBH than low SBH. This could then explain why Φ_{CV} was higher than predicted in the mean barrier height model that presumes a Gaussian distribution.

IV. CONCLUSIONS

We have demonstrated n-n Ge/SiC heterojunction Schottky barrier diodes operating in a range of temperatures from -50^{o}C to 175^{o}C. The characterisation of the diodes has revealed inhomogeneity at the interface, despite near ideal characteristics ($n < 1.05$) at 25^{o}C. With ohmic front and back contacts, the Ge/SiC heterojunction was the only contributor to the Schottky behaviour. In attempting to linearise the Richardson plots, two techniques that had previously been applied to inhomogeneous metal-semiconductor Schottky barriers were applied to the inhomogeneous Ge/SiC heterojunction. Accurate values of A^{**} were extracted from methods that also bore Φ_{eff} and Φ_0, SBH values analogous to those produced from I-V and C-V analyses respectively. However, the SBH attained from C-V analyses did not correlate with the mean SBH as expected. In the future, we would like to further analyse the Ni/Ge/SiC junctions through the use of transmission electron microscopy.

[1] A. Agarwal, R. Singh, S.-H. Ryu, J. Richmond, C. Capell, S. Schwab, B. Moore and J. Palmour, *www.cree.com* (2008).

[2] P. M. Gammon, A. Pérez-Tomás, M. R. Jennings, G. J. Roberts, M. C. Davis, V. A. Shah, S. E. Burrows, N. R. Wilson, J. A. Covington, and P. A. Mawby *Appl. Phys. Lett.* **93**, 112104 (2008).

[3] A. Pérez-Tomás, P. Brosselard, J. Hassan, X. Jordà, P. Godignon, M. Placidi, A. Constant, J. Millán and J. P. Bergman, *Semicond. Sci. Technol.* **23**, 125004 (2008).

[4] A. Pérez-Tomás, M. R. Jennings, M. Davis, V. Shah, T. Grasby, J. A. Covington and P. A. Mawby, *Microelectronics Journal*, **38**, 1233 (2007).

[5] A. Pérez-Tomás, M. R. Jennings, M. Davis, J. A. Covington, P. A. Mawby, V. Shah and T. Grasby, *J. Appl. Phys.* **102** 014505 (2007).

[6] M. R. Jennings, A. Pérez-Tomás, O. J. Guy, R. Hammond, S. E. Burrows, P. M. Gammon, M. Lodzinski, J. A. Covington, and P. A. Mawby, *Electrochemical and Solid-State Letters*, **11**, H306 (2008).

[7] L. Chen, O. J. Guy, M. R. Jennings, P. Igic, S. P. Wilks and P. A. Mawby, *Solid-State Electronics*, **51**, 662 (2007).

[8] M. E. Aydin, N. Yildirim and A. Türüt, *J. Appl. Phys.*, **102**, 043701 (2007).

[9] J. H. Werner and H. H. Güttler, *J. Appl. Phys.* **69**, 1522 (1991).

[10] F. Roccaforte, F. La Via, V. Raineri, R. Pierobon, and E. Zanoni, *J. Appl. Phys.*, **93**, 9137 (2003).

[11] R. T. Tung, *Phys. Rev. B*, **45**, 13509 (1992).

[12] J. P. Sullivan, R. T. Tung, M. R. Pinto and W. R. Graham, *J. Appl. Phys.*, **70**, 127403 (1991).

[13] R. T. Tung, *Appl. Phys. Lett.*, **58**, 2821 (1991).

[14] J. L. Freeouf, T. N. Jackson, S. E. Laux, and J. M. Woodall, *J. Vac. Sci. Technol.*, **21**, 2570 (1982).

[15] Y. P. Song, R. L. Van Meirhaeghe, W. H. Laflère and F. Cardon, *Solid-State Electronics*, **29**, 633 (1986).

[16] F. Iucolano, F. Roccaforte, F. Giannazzo, and V. Raineri, *J. Appl. Phys.* **102**, 113701 (2007).

[17] R. F. Schmitsdorf, T. U. Kampen, and W. Mönch, *J. Vac. Sci. Technol. B*, **15**, 4 1221 (1997).

[18] S. Chand and S. Bala, *Semicond. Sci. Technol.*, **20**, 1143 (2005).

[19] H. J. Im, Y. Ding, J. P. Pelz and W. J. Choyke, *Phys. Rev. B*, **64**, 075310, (2001).

[20] F. Giannazzo, F. Roccaforte, V. Raineri and S. F. Liotta, *Europhys. Lett.*, **74** (4), 686 (2006).

[21] F. A. Padovani and G. G. Sumner, *J. Appl. Phys.*, **36**, 3744 (1965).

[22] G. Eftekhari, B. Tuck and D. De Cogan, *J. Phys. D: Appl. Phys.*, **16**, 1099 (1983).

[23] A. S. Bhuiyan, A. Martinez and D. Esteve, *Thin Solid Films*, **161** 93 (1988).

[24] I. Ohdomari and K. N. Tu, *J. Appl. Phys.*, **51**, 3735 (1980).

[25] W. Kern, and D. A. Poutinen, *RCA Rev.* **31**, 187 (1970).

[26] W. T. Anderson, A. Christou and J. E. Davey, *IEEE J. Solid-State Circ.*, **SC13**, 4430, (1978).

[27] F. A. Padovani and R. Stratton, *Solid-State Electronics*, **9**, 695 (1966).

[28] C.R. Crowell, *Solid-State Electronics*, **12**, 55 (1969).

[29] D. K. Schroder, *Semiconductor Material and Device Characterization*, p. 158 (Wiley, New York, 1998).

[30] S. M. Sze, *Physics of Semiconductor Devices*, (Wiley, New York, 1981).

[31] G. S. Marlow and M. B. Das, *Solid-Store Electronics* **25**, 291 (1982).

[32] I. P. Nikitina, K. V. Vassilevski, N. G. Wright, A. B. Horsfall, A. G. ONeill and C. M. Johnson, *J. Appl. Phys.*, **97**, 083709 (2005).

[33] A. Itoh, T. Kimoto, and H. Matsunami, *IEEE Electron. Device Letters*, **16**, 6280 (1995).

[34] C. F. Pirri, S. Ferrero, L. Scaltrito, D. Perrone, S. Guastella, M. Furno, G. Richieri and L. Merlin, *Microelectronic Engineering*, **83**, 86 (2006).

[35] A. M. Goodman, *J. Appl. Phys.* **34**, 329 (1963).

[36] F. Roccaforte, F. La Via, A. Baeri, V. Raineri, L. Calcagno and F. Mangano, *J. Appl. Phys.*, **96**, 4134 (2004).

[37] M. R. Jennings, A. Pérez-Tomás, M. Davies, D. Walker, L. Zhu, P. Losee, W. Huang, S. Balachandran, O. J. Guy, J. A. Covington, T. P. Chow and P. A. Mawby, *Solid-State Electronics*, **51**, 797 (2007).